European Journal of Physics

PAPER

Studying the hyperfine interaction using the variational quantum eigensolver

A J Martin and J W Martin
Department of Physics, The University of Winnipeg, Winnipeg, MB, R3B 2E9, Canada
E-mail: j.martin@uwinnipeg.ca

OPEN ACCESS

RECEIVED
14 October 2025

REVISED
9 February 2026

ACCEPTED FOR PUBLICATION
23 February 2026

PUBLISHED
25 March 2026

Keywords: hyperfine structure, atomic physics, variational quantum mechanics, quantum computing, variational quantum eigensolver

Abstract

An exciting application of quantum computers is the simulation of physical systems. The goal of the variational quantum eigensolver (VQE) is to approximate the ground state of a quantum system. This is done by applying the variational principle, finding the expectation value of the Hamiltonian in an ansatz quantum state, then minimizing this expectation value with respect to the parameters of the ansatz. In the VQE, the calculation of the expectation value in the ansatz state is done on a quantum computer, while the adjustment of the parameters of the ansatz to find the minimum energy is done classically. In this article we study the spin–spin coupling $H = A\vec{S_1}\cdot\vec{S_2}$. This coupling appears in the hyperfine interaction of atomic systems, resulting from the interaction of the electronic spin with the nuclear spin. The form of the interaction satisfies the requirements of the VQE, that the Hamiltonian must be expressed as sums of products of Pauli matrices, making it an interesting trial system for a quantum computer. In our calculation technique, the expectation value is implemented using two qubits on a quantum computer. The ansatz state is simplified to a single free parameter, which is then optimized classically. The algorithm converges rapidly, and the correct ground state is deduced. This serves as a useful example of implementing the VQE to solve a physically realizable problem in quantum mechanics.

1. Introduction

The hyperfine interaction is responsible for splittings in atomic energy levels. In alkali atoms (e.g. Na, K, Rb, and Cs), the typical hyperfine splitting of the ground state ($^{2S+1}L_J = {}^2S_{1/2}$) is 1–10 GHz, and the typical hyperfine splitting of the laser-accessible fine-structure states ($^2P_{1/2}$ and $^2P_{3/2}$) are a few hundred MHz. The gives a rich structure even considering the typical Doppler broadening of ∼1 GHz, and makes the splittings easy to observe with typical diode lasers (whose natural linewidths can be of order kHz or less) [1].

In the present work, we have set out to study the hyperfine interaction using quantum computers. We used an algorithm based on the variational principle, the variational quantum eigensolver (VQE) [2], to study its ability to find the ground state of a hyperfine Hamiltonian. This serves as a useful example of implementing the VQE on a two-qubit system, which can be generalized to more complicated Hamiltonians.

VQE has been shown to be a feasible algorithm for existing and near-term quantum computers. The method has generated a wealth of literature [3] aimed at utilizing, expanding, and improving the algorithm. Mapping fermionic basis states to the quantum computational basis, and the development of ansatz states are key issues that have been investigated [4].

Variational quantum algorithms are a potentially promising solution to classically intractable quantum chemistry and physics problems, with potential applications in solid-state physics such as high temperature superconductivity [5]. It is broadly thought to be an algorithm that could be implemented in noisy intermediate state quantum (NISQ) hardware, that could eventually demonstrate an advantage over classical algorithms [6, 7]. Variational Quantum algorithms are also applicable when calculations of molecular excited states must be performed [2, 8, 9].

There is also a relationship between quantum machine learning algorithms and variational quantum algorithms [3, 7]. A feature of VQE is the minimization of an expectation value, which bears a striking similarity to the minimization of a cost function in machine learning. For this reason, the expectation value is sometimes referred to as the cost function, borrowing the terminology from the field of quantum machine learning.

This paper presents an example of a simple two-spin Hamiltonian with a well-known solution. We then implement the VQE algorithm using the two-spin system as an example. We develop a physically motivated ansatz which can be easily encoded using standard quantum gates. Statistics of measurements on each term in the Hamiltonian are then acquired in order to calculate the expectation value of the overall Hamiltonian. This is done using freely available quantum computing resources of the IBM Quantum Platform [10]. The classical computer portion of the calculation is done in the first instance by manually sweeping the free parameter of the ansatz state, and in the second instance using the Qiskit toolkit to perform the optimization using a classical algorithm.

2. The variational principle

The variational principle and its application to quantum mechanics is covered in most introductory quantum mechanics textbooks [11, 12]. It is based on the fact that the expectation value of the Hamiltonian H in any normalized quantum state $|\psi\rangle$ is always larger than the ground state energy $E_{\rm gs}$, i.e.

$$E_{\rm gs} \leqslant \langle\psi|H|\psi\rangle \equiv \langle H\rangle. \tag{1}$$

This is often used to find the approximate value of the ground state energy of a system, by trying a parameterized ansatz for the ground state wavefunction. By varying the parameters of the ansatz, a minimum energy may be found.

Let the ansatz state $|\psi(\theta)\rangle$ have a set of parameters $\theta = (\theta_1, \theta_2, \ldots, \theta_N)$. The minimum energy then obeys

$$\left.\frac{\partial <H>}{\partial \theta_i}\right|_{\theta_{\rm min}} = 0 \qquad \forall\ i = 1,\ldots,N. \tag{2}$$

The energy $E_{\rm min} = <H>|_{\theta_{\rm min}}$ is taken to be an approximation of the ground state energy, and the wavefunction $|\psi(\theta_{\rm min})\rangle$ is an approximation of the ground state wavefunction. In introductory texts, the ansatz state and expectation value of the Hamiltonian can be calculated analytically. Differentiation is also done analytically to find the best set of parameters $\theta_{\rm min}$ resulting in the minimum energy and the corresponding wavefunction.

The variational principle has been applied to problems in molecular physics, condensed matter physics, solid state physics, nuclear physics, and chemistry. The Hartree–Fock method and Density Functional Theory are examples of variational methods.

The VQE algorithm [2] implements the variational method using a quantum computer, combined with an optimization step done using a classical computer. The calculation of the expectation value of the Hamiltonian in the ansatz state is done using the quantum computer. Parameters of the ansatz state are then adjusted by the classical computer. The process is repeated until a minimum expectation value has been reached.

3. The hyperfine interaction

Fine structure of alkali atoms results from a combination of spin–orbit coupling and relativistic effects. The much smaller hyperfine structure results from the interaction of the orbiting electron with the dipole magnetic field of the atomic nucleus. In alkali atoms, the hyperfine contribution to the Hamiltonian can be approximated as [13]

$$H = A\overrightarrow{I}\cdot\overrightarrow{J}, \tag{3}$$

where $\overrightarrow{I}$ is the nuclear spin and $\overrightarrow{J}$ the total angular momentum of the electron (spin plus orbital). The factor A can be calculated using the electron's radial wavefunction. Generally, the factor A is fitted to data [14].

When higher spin systems are taken into account, additional corrections arise due to couplings to the nuclear electric quadrupole and magnetic octupole moments. For instance, the nuclear magnetic octupole moment of ^{133}Cs ($I = 7/2$) has been measured by considering these higher order corrections [15].

In the case of a spin-1/2 nucleus, with the electron orbital angular momentum $L = 0$, equation (3) would be sufficient, and would contain a dot product of the nuclear spin and the electron spin. In the following, we consider a Hamiltonian of this form, which is suitable for application of the VQE technique, in part because it can easily be written in terms of Pauli matrices. In section 6, we present the exact solution for this Hamiltonian, and in subsequent sections, we present solutions using the VQE algorithm on quantum computers.

4. Quantum computing

Quantum computers [16–18] are an emerging new paradigm for complex computations. They use the principles of quantum mechanics and innovative algorithms to potentially accelerate computations beyond what is possible with classical computers, which are inherently limited by Moore's Law.

Rather than encoding information in bits, a quantum computer encodes information in qubits. Each qubit's wavefunction can be written as

$$|\psi\rangle = \alpha|0\rangle + \beta|1\rangle \tag{4}$$

with α and β complex and subject to $|\alpha|^2 + |\beta|^2 = 1$. Thus each qubit may be placed in a superposition of $|0\rangle$ and $|1\rangle$. Computation proceeds via unitary operations on the set of qubits. Operators that connect the qubits can be used to generate entanglement. This enables the set of qubits in the computer to be placed in states of increasing complexity. For example, a superposition of all possible binary inputs can be encoded in a straightforward fashion. The principles of superposition, entanglement, and interference are used in quantum algorithms to speed computation.

In the following description, we make use of quantum circuit diagrams to explain algorithms. These explain the preparation of the state of the qubits through the computation, the unitary operations which modify the state of the qubits, and end with the measurement of each qubit, from which results are inferred. We refer the reader to introductory texts on quantum computation for a review of quantum circuit diagrams, and the typical unitary operators encountered in quantum computation [16–18].

An exciting application of quantum computers is the simulation of physical quantum-mechanical systems. Since these systems are quantum mechanical, it is anticipated that quantum computers will naturally lead to a performance gain relative to classical computers. The VQE is an algorithm which has demonstrated successes in the solution of physical systems [2]. It is naturally suited to solving systems involving spin degrees of freedom, as shall now be described.

5. The concept of the variational quantum eigensolver

In order to use the VQE, the Hamiltonian H must be expressed as a sum of products of Pauli matrices [2]

$$H = \sum_{i\alpha} h^i_\alpha \sigma^i_\alpha + \sum_{ij\alpha\beta} h^{ij}_{\alpha\beta} \sigma^i_\alpha \sigma^j_\beta + \ldots \tag{5}$$

where the coefficients $h \in \mathbb{R}$, and the Greek indices indicate different Pauli matrices $(\alpha, \beta, \ldots) \in \{x, y, z\}$. The Roman indices $i, j, \ldots$ indicate the subsystem acted upon. For instance, in a system of N stationary spin-1/2 particles, $i, j, \ldots$ would, in general, run from 1 to N, and the expansion would terminate with products of N Pauli matrices.

As shall become clear from our example (section 6), this decomposition allows the Hamiltonian to be broken down easily into measurable components when encoded on a quantum computer.

Each term in the Hamiltonian contains products of Pauli matrices, and these terms are added together. We recast equation (5) and label each of these terms in the Hamiltonian with a superscript in parentheses

$$H = \sum_i H^{(i)} \tag{6}$$

where in this case the sum is over all terms in the expansion.

The VQE algorithm (figure 1) proceeds by encoding an ansatz state $|\psi(\theta)\rangle$ on the required number of qubits. For instance, if the Hamiltonian was describing the interactions of the spins of N static spin-1/2 particles, N qubits would be required. The spin state of each particle would be represented by the quantum state of the corresponding qubit. The quantity θ represents a set of parameters which will be freely adjusted in order to minimize the expectation value of the Hamiltonian. As in variational quantum mechanics, a good ansatz should have a limited number of parameters, but enough parameters to approximate the unknown ground state wavefunction effectively.

Multiple measurements of each term in the Hamiltonian $H^{(i)}$ are performed on the quantum computer to estimate expectation values. To measure the expectation value of H, measurements are performed by rotating to the basis where each term is diagonal. For instance, if the Hamiltonian contains σ_x, the corresponding qubit is rotated to the basis where σ_x is diagonal before measurement. This will be discussed further in section 7.

This process is repeated for each term of the Hamiltonian, and the results are then collected on a classical computer. The classical computer aggregates the measurement results with the appropriate prefactors $h^{ij\ldots}_{\alpha\beta\ldots}$ to calculate the expectation value of the Hamiltonian

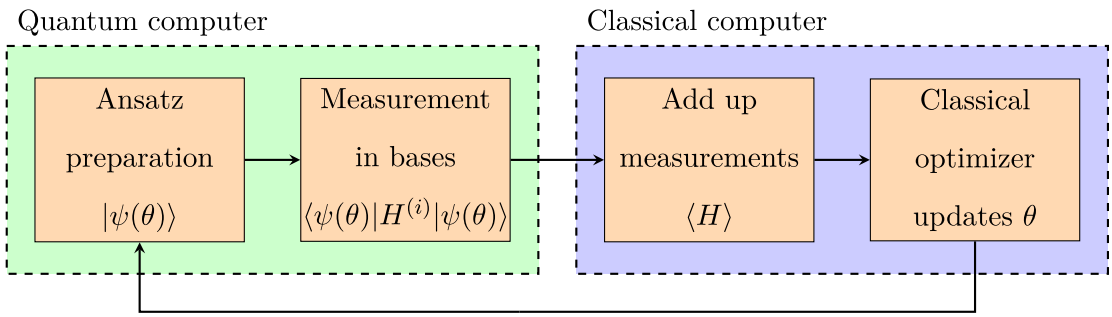

Figure 1. Concept of the variational quantum eigensolver.

$$\langle\psi(\theta)|H|\psi(\theta)\rangle = \sum_i \langle\psi(\theta)|H^{(i)}|\psi(\theta)\rangle. \tag{7}$$

Subsequently, the classical computer adjusts the parameters θ of the ansatz state and sends the new set of parameters to the quantum computer for another round of measurements. This process continues, using a classical optimization algorithm to iteratively minimize the expectation value of the Hamiltonian, thereby finding the best estimate of the ground state wavefunction and its corresponding energy.

One of the key issues for the VQE is the development of an ansatz that is a balance of having few parameters while yet adequately describing the ground state. Having too many parameters would affect the performance of the classical optimization procedure, while not having enough would lead to inadequate approximation of the true ground state. The interplay of variational quantum mechanics and machine learning has led to many ideas of how best to tackle this problem [3].

We now proceed to describe our simple two-qubit model that will illustrate the concept of the VQE, and is easy to implement on a quantum computer.

6. Hyperfine Hamiltonian and exact solution

The form of the hyperfine (spin–spin) Hamiltonian for an electron in an $L = 0$ orbital interacting with a spin-1/2 nucleus is

$$H = A\vec{S}^1 \cdot \vec{S}^2 = A(S_x^1 S_x^2 + S_y^1 S_y^2 + S_z^1 S_z^2) \tag{8}$$

where $\vec{S}^i$ is the spin vector of particle i and A is a constant. The spin vectors $\vec{S}^{1,2}$ are operators, corresponding to the nuclear (1) and electron (2) spins. In nonrelativistic quantum mechanics, each spin vector operator can be represented as a vector of Pauli matrices

$$\vec{S} = \frac{\hbar}{2}\vec{\sigma} \tag{9}$$

in the two-dimensional spinor space of each particle. The Hamiltonian satisfies the requirement of VQE that the Hamiltonian be written as a sum of products of Pauli matrices

$$H = \alpha\vec{\sigma}^1 \cdot \vec{\sigma}^2 = \alpha(\sigma_x^1\sigma_x^2 + \sigma_y^1\sigma_y^2 + \sigma_z^1\sigma_z^2) \tag{10}$$

where $\alpha = A\hbar^2/4$ would have units of energy.

On a quantum computer, the Hamiltonian is encoded as a sum of tensor products of operators acting on two qubits. Switching notation to a more common one for quantum computers, we write

$$H = \alpha(\sigma_x \otimes \sigma_x + \sigma_y \otimes \sigma_y + \sigma_z \otimes \sigma_z) = \alpha(X \otimes X + Y \otimes Y + Z \otimes Z) \tag{11}$$

where the first operator in each tensor product would be applied to qubit 1 (the electron spin qubit) and the second operator to qubit 2 (the nuclear spin qubit).

The exact solutions for the energy eigenstates of the Hamiltonian in equation (8) are straightforward to find. The solutions are eigenstates of the total spin operator squared

$$S^2 = (\vec{S}^1 + \vec{S}^2)^2 = (\vec{S}^1)^2 + (\vec{S}^2)^2 + 2\vec{S}^1 \cdot \vec{S}^2. \tag{12}$$

This can be rearranged to isolate the main term in the Hamiltonian, $\vec{S}^1 \cdot \vec{S}^2$, as

$$\vec{S}^1 \cdot \vec{S}^2 = \frac{1}{2}\left(S^2 - (\vec{S}^1)^2 - (\vec{S}^2)^2\right). \tag{13}$$

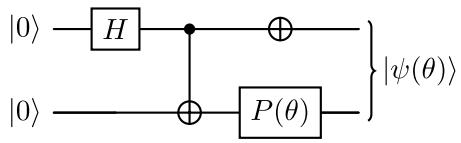

Figure 2. Quantum circuit which prepares the ansatz state $|\psi(\theta)\rangle$.

The smallest eigenvalues of S^2 correspond to when the two spin-1/2 particles occupy the singlet configuration ($s=0$) where the spins are antiparallel and carry a total spin of 0

$$|s_1 s_2;\, sm\rangle = |\tfrac{1}{2}\tfrac{1}{2};\, 00\rangle = \frac{1}{\sqrt{2}}(|01\rangle - |10\rangle). \tag{14}$$

Here, the factors $\frac{1}{\sqrt{2}}$ and $-\frac{1}{\sqrt{2}}$ are Clebsch–Gordan coefficients, needed for the transformation from the basis of the individual spin z-components (known as the computational basis in quantum computing) to the basis of total spin and its z-component.

Acting on this state with $\overrightarrow{S}^1 \cdot \overrightarrow{S}^2$, we find

$$\overrightarrow{S}^1 \cdot \overrightarrow{S}^2 |\tfrac{1}{2}\tfrac{1}{2};\, 00\rangle = \frac{1}{2}\left(0(0+1)\hbar^2 - \frac{1}{2}(\frac{1}{2}+1)\hbar^2 - \frac{1}{2}(\frac{1}{2}+1)\hbar^2\right)|\tfrac{1}{2}\tfrac{1}{2};\, 00\rangle = -\frac{3}{4}\hbar^2 |\tfrac{1}{2}\tfrac{1}{2};\, 00\rangle. \tag{15}$$

Therefore, the ground state energy for our Hamiltonian is

$$E = A\left(-\frac{3}{4}\hbar^2\right) = -\frac{3A\hbar^2}{4} = -3\alpha. \tag{16}$$

We will henceforth set $\alpha = 1$, so that the ground state found using VQE will approximate the theoretical ground state energy $E = -3$. We now proceed to discover the ground state using the VQE algorithm.

7. Calculating the expectation value on a quantum computer

7.1. Preparation of a simple ansatz state

To calculate the expectation value, we first need to prepare an ansatz state for our Hamiltonian. For the purposes of this example, we choose the simple ansatz

$$|\psi(\theta)\rangle = \frac{1}{\sqrt{2}}(|01\rangle + e^{i\theta}|10\rangle) \tag{17}$$

where θ is now a single (real) free parameter.

While a selection with more free parameters is possible, this state is well motivated physically by the structure of the Hamiltonian. The states $|00\rangle$ and $|11\rangle$ are stretched states, representing spins that are parallel to one another. We would expect such states to have a larger (more positive) value of $\overrightarrow{S}^1 \cdot \overrightarrow{S}^2$, compared to the states $|01\rangle$ and $|10\rangle$, where the spins point antiparallel to one another. A linear combination of $|01\rangle$ and $|10\rangle$ would therefore be motivated by the individual terms having generally smaller values of $\overrightarrow{S}^1 \cdot \overrightarrow{S}^2$. The most arbitrary possible linear combination that always remains properly normalized is given by equation (17). A quantum circuit that prepares this ansatz state is shown in figure 2.

In the preparation of the ansatz state, we have used a phase gate

$$P(\theta) = \begin{pmatrix} 1 & 0 \\ 0 & e^{i\theta} \end{pmatrix} \tag{18}$$

to generate the arbitrary phase between the two terms in equation (17). We now need to use the quantum computer to calculate the expectation value of the various terms in the Hamiltonian.

7.2. Finding the expectation value of a tensor product of Pauli matrices on a quantum computer

The process of measuring the expectation value of the various terms in the Hamiltonian using a quantum computer involves preparing the ansatz state, measuring in the appropriate basis, and then repeating this process to build up statistics on the expectation value. For this discussion, let us suppose that the state of the two qubits is an arbitrary state $|\psi\rangle$, and that we desire to make a measurement of the expectation value of each piece of the Hamiltonian in equation (11).

Because $Z \otimes Z$ is diagonal in the computational basis, no basis transformation is necessary. One way to see this is as follows. Suppose the state is measured, and the result $|01\rangle$ is found. This would mean that the first

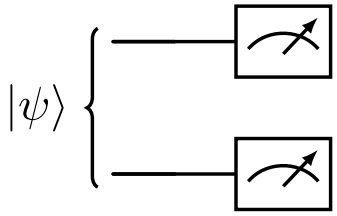

Figure 3. Circuit for measuring $\langle Z \otimes Z \rangle$.

qubit was found in the state $|0\rangle = \begin{pmatrix}1\\0\end{pmatrix}$ and the second qubit in the state $|1\rangle = \begin{pmatrix}0\\1\end{pmatrix}$. These are eigenstates of the $Z = \begin{pmatrix}1 & 0\\0 & -1\end{pmatrix}$ operator; they have perfectly well defined values of the observable Z. For the first qubit, the eigenvalue is $+1$, while for the second qubit, the eigenvalue is -1. The result for the measurement of $Z \otimes Z$ is therefore $(+1)(-1) = -1$.

In a similar way, the repeated preparation and measurement of a two qubit state $|\psi\rangle$ in the computational basis would result in

$$\begin{aligned}\langle Z \otimes \ Z \rangle = & P_{00} \cdot (+1)(+1) \\ & + P_{01} \cdot (+1)(-1) \\ & + P_{10} \cdot (-1)(+1) \\ & + P_{11} \cdot (-1)(-1)\end{aligned} \tag{19}$$

where P_{ij} is the probability to find the qubits in the state $|ij\rangle$. The correct circuit to make this measurement is therefore very simple (figure 3).

The result of each measurement will be either $+1$ or -1 for each qubit. The results will occur with different probabilities, depending on the state $|\psi\rangle$. If we always prepare the same state $|\psi\rangle$ and feed it into the measurement, we can repeatedly run this circuit, building up results for the probabilities and use equation (19) to find the expectation value.

To measure $X \otimes X$, the probabilities to find the qubits in the states $|+\rangle = \frac{1}{\sqrt{2}}\begin{pmatrix}1\\1\end{pmatrix}$ and $|-\rangle = \frac{1}{\sqrt{2}}\begin{pmatrix}1\\-1\end{pmatrix}$ are needed. These are eigenstates of the X operator

$$\begin{aligned}X|+\rangle &= (+1)|+\rangle \\ X|-\rangle &= (-1)|-\rangle.\end{aligned} \tag{20}$$

If the two-qubit state $|\psi\rangle$ were found to be in the state $|+-\rangle$, its $X \otimes X$ value would be $(+1)(-1) = -1$. In a similar way to equation (19), assuming we could find the probabilities in the X basis, we could then determine the expectation value

$$\begin{aligned}\langle X \otimes \ X \rangle = & P_{++} \cdot (+1)(+1) \\ & + P_{+-} \cdot (+1)(-1) \\ & + P_{-+} \cdot (-1)(+1) \\ & + P_{--} \cdot (-1)(-1).\end{aligned} \tag{21}$$

In order to measure the required probabilities in this case, we need an operator that transforms $|+\rangle$ into $|0\rangle$ and $|-\rangle$ into $|1\rangle$, i.e. we need to transform to the X basis. Fortunately, the Hadamard operator does this! So, to measure the required probabilities, we apply a Hadamard gate to both qubits (figure 4).

Suppose that $|\psi\rangle = |+-\rangle$ is fed into the circuit. After the Hadamards, the state of the system will be $|01\rangle$ and $+1$ will be measured for the first qubit and -1 for the second. Thus, the probability of finding $|+-\rangle$ will be reported as $|01\rangle$, and so on.

Another way that this can be understood is to imagine the state $|+\rangle$ as a spin pointing along the $+x$-direction in three dimensional space. We need to rotate this spin to point along the $+z$-direction (a state we call $|0\rangle$) before we measure it to find probabilities. There is another operator (besides the Hadamard operator) which can achieve this: the rotation gate $R_y(-\pi/2)$. Thus an alternative circuit which would give the same result would employ rotation gates instead of Hadamard gates (figure 5).

Both these circuits (figures 4 and 5) can be shown to correctly measure the probabilities required for equation (21).

Finally, the term $\langle Y \otimes Y \rangle$ must be measured. Similar to the previous case, the strategy is to transform from the Y basis

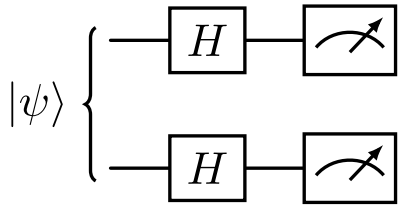

Figure 4. Circuit for measuring $\langle X \otimes X \rangle$.

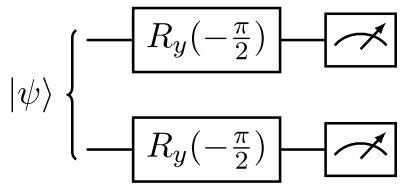

Figure 5. Alternative circuit for measuring $\langle X \otimes X \rangle$.

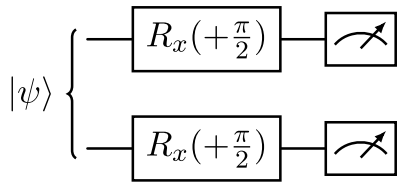

Figure 6. Circuit for measuring $\langle Y \otimes Y \rangle$.

$$Y|+_y\rangle = (+1)|\ +_y\ \rangle$$
$$Y|-_y\rangle = (-1)|\ -_y\ \rangle \tag{22}$$

to the Z basis, before making the measurement. The simplest transformation that achieves this can be deduced from a similar line of argumentation as the rotation gate discussion of the X basis case. Imagine the state $|+_y\rangle$ as a spin pointing along the $+y$-direction. In order to transform this state into a spin pointing along the $+z$-direction ($|0\rangle$), a rotation of $+\pi/2$ about the x-axis would be required. That is, the correct transformation is $R_x(+\pi/2)$.

The quantum circuit diagram for this measurement may be found in figure 6.

The basic reason for the VQE algorithm requiring the Hamiltonian to be a product of Pauli matrices should now be evident. Any product of Pauli matrices would simply require the correct rotation to be applied to the relevant qubit, in order to be measured.

8. Implementation on a quantum computer

8.1. Setup and results using a simulated quantum computer

Implementation of the algorithm in the IBM quantum composer [19] is achieved through the preparation of three quantum circuits (figure 7), one each to measure $\langle X \otimes X \rangle$, $\langle Y \otimes Y \rangle$, and $\langle Z \otimes Z \rangle$. The quantum composer is a free-to-use interface, where programming is done graphically by dragging and dropping circuit elements to create the desired quantum circuit diagram. Once implemented using the graphical programming utility, the probabilities can be measured using either the included simulator, or by transpiling and sending jobs to a quantum computer.

The VQE algorithm is demonstrated in the following way. Since the ansatz $|\psi(\theta)\rangle$ (equation (17)) has only one free parameter, it can be selected at random. We start with the guess that $\theta = 1$ (radians). The value for θ is entered into each of the circuits of figure 7, and the probabilities are calculated (using either the simulator or an available quantum computer, depending on the time available). With the probabilities of each state measured, the mean values of each term in the Hamiltonian are calculated (via the equations in figure 7), and the results

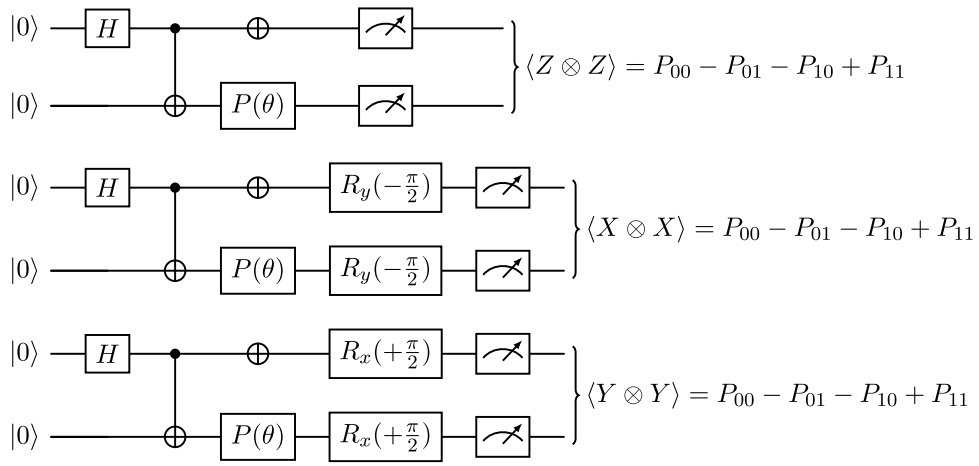

Figure 7. Scheme of implementation in the IBM quantum composer involving three quantum circuits.

Table 1. Results from the IBM quantum composer. Results are from 1024 shots on a simulated quantum computer.

θ (radians)	$\langle Z\otimes Z\rangle$	$\langle X\otimes X\rangle$	$\langle Y\otimes Y\rangle$	E (sum)
1	−1.00	0.48	0.48	−0.04
0	−1.00	1.00	1.00	1.00
$\pi/2$	−1.00	0.00	0.00	−1.00
2	−1.00	−0.46	−0.46	−1.92
3	−1.00	−0.99	−0.99	−2.98
π	−1.00	−1.00	−1.00	−3.00
4	−1.00	−0.71	−0.71	−2.42

summed to arrive at the energy. Sample results are presented in table 1 (which came from the simulator). The resultant energy is $E=-0.04$.

Next, another value for θ is chosen. We select $\theta=0$, manually change the value in the phase gate in each quantum circuit, calculate the probabilities, and fill in the next row in table 1. In this case, we find $E=1.00$. Our goal is to adjust θ until the energy is *minimized*, so obviously we have gone in the wrong direction, in this case.

The process is repeated until the optimum value for θ which minimizes energy is found (see the remaining rows in table 1). As expected, the minimized value of $E=-3.00$ appears as θ is adjusted toward odd multiples of π. Thus we have demonstrated the principle of the VQE algorithm in its ability to find the minimum energy for this Hamiltonian.

8.2. Using a real quantum computer

The following measurement results (figures 8, 9 and 10) were obtained using 2000 repeated measurements using the Sampler V2 primitive on ibmq_brisbane v1.1.31, which was one of the IBM Quantum Eagle r3 processors. For this example, the value $\theta=\pi/2$ was used in the preparation of the ansatz state. This choice of θ is not the optimal parameter choice for discovering the ground state; it is provided as an example.

The results are noisier than the simulated results, as might be expected. Figure 8 results in $\langle Z\otimes Z\rangle=-0.88$, figure 9 gives $\langle X\otimes X\rangle=0.03$, and figure 10 gives $\langle Y\otimes Y\rangle=0.04$, resulting in $E=-0.81$. Considering the noise, this agrees well with the expected value $E=-1$ for $\theta=\pi/2$ (table 1). We conduct a more detailed analysis of noise and errors in the next section.

While it is possible to conduct more experiments using the real quantum computer, this becomes tedious if submitting each job manually from the quantum composer.

8.3. Implementation using Qiskit to iteratively find the ground state

We provide an implementation using Qiskit [20], which gives access to the quantum computers in a more automated and efficient fashion.

Figure 11 shows the VQE convergence plot for $\langle X\otimes X+Y\otimes Y+Z\otimes Z\rangle$, implemented in python [21] and executed on ibmq_fez v1.3.30, which is one of the Heron r2 processors. The algorithm used Bound

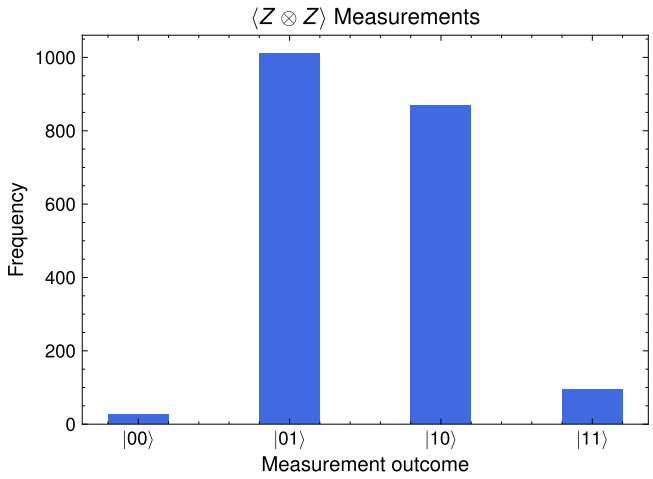

Figure 8. $\langle Z \otimes Z \rangle$ measurement outcomes in the computational basis for parameter $\theta = \pi/2$ radians.

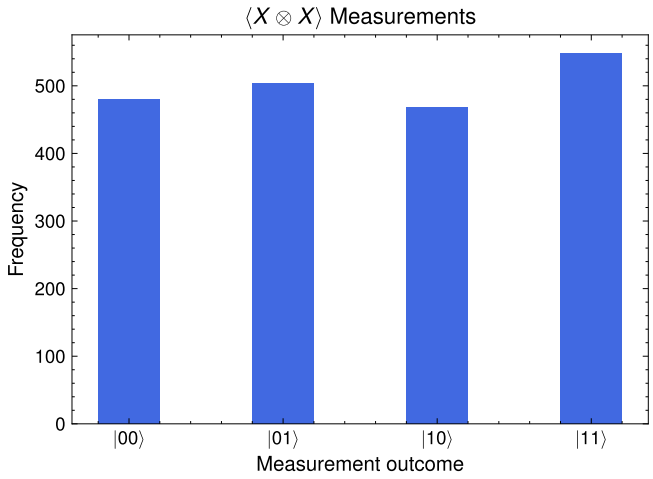

Figure 9. $\langle X \otimes X \rangle$ measurement outcomes in the computational basis for parameter $\theta = \pi/2$ radians.

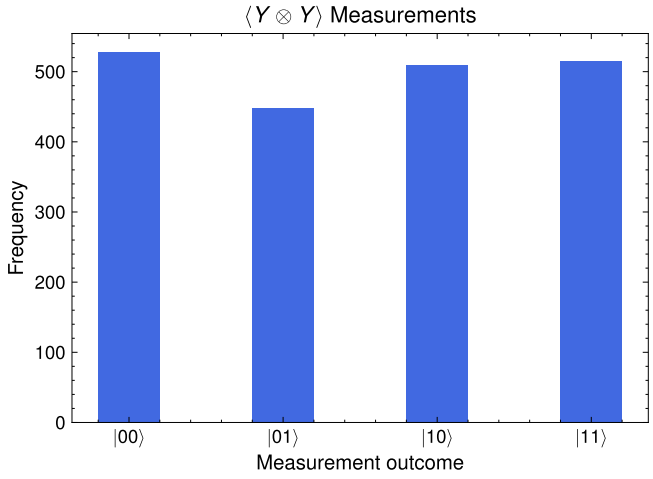

Figure 10. $\langle Y \otimes Y \rangle$ measurement outcomes in the computational basis for parameter $\theta = \pi/2$ radians.

Optimization BY Quadratic Approximation (BOBYQA) [22] to optimize the ansatz parameter, and successfully converged to the minimum energy (being 2% lower than the average expectation value, compared to the theoretical ground state of −3.00) after 16 iterations. The 2% error in the approximated ground state energy

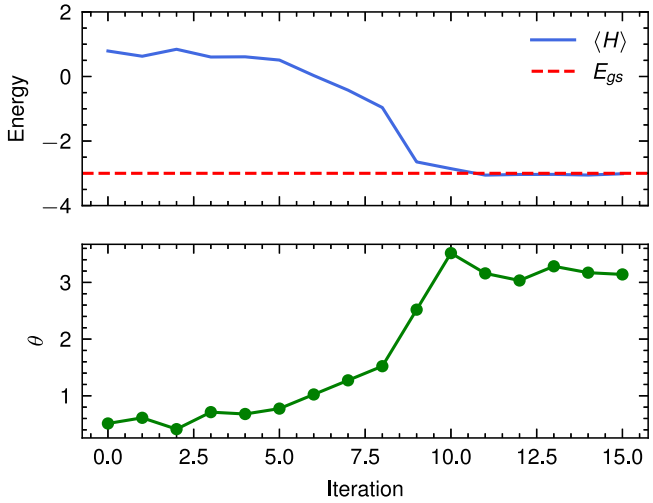

Figure 11. VQE convergence plot for $\langle H\rangle = \langle X\otimes X + Y\otimes Y + Z\otimes Z\rangle$, implemented on an IBM Heron r2 QPU and optimized using BOBYQA. The second plot shows the parameter value at each iteration. Each point represents an average of 2042 shots.

Table 2. Qubit 131 and 132 properties. Exhaustive calibration data for all qubits may be found in the experiment repository [21].

Qubit	T_1 (μs)	T_2 (μs)	t_{1Q} (ns)	t_{2Q} (ns)	Readout error	CZ error	SX error	X error
131	170.43	174.55	24	68	8.53×10^{-2}	1.55×10^{-3}	1.41×10^{-4}	1.41×10^{-4}
132	161.48	167.30	24	68	6.83×10^{-3}	1.55×10^{-3}	1.83×10^{-4}	1.83×10^{-4}

might be reduced by increasing the number of iterations—either manually, or by increasing the convergence tolerance of the classical optimizer.

The use of BOBYQA is appropriate for noisy systems such as NISQ devices. Stochastic gradient approximation algorithms are widely used in VQE. A prime example of this is the simultaneous perturbation stochastic approximation (SPSA) method, which estimates gradients with only two objective function evaluations, independent of parameter dimension [23]. SPSA would be expected to outperform BOBYQA for more degrees of freedom.

This VQE experiment was conducted on two of fez' qubits, 131 and 132, as indicated on the IBM Quantum Platform. To quantify the impact of hardware noise on the variational energy estimate (figure 11), we utilized the device calibration data relevant at the time of execution. A list of data for qubits 131 and 132 is shown in table 2. No resonant frequencies or anharmonicities were reported for either qubit.

We performed an analysis of the ansatz decoherence limits by comparing the total circuit duration to the qubit relaxation times (T_1, T_2). Circuit timing can be visualized by using the circuit timing functions within Qiskit, or manually determined by computing gate times using the calibration data. We will utilize the latter to determine the probability that an error will occur within circuit execution time.

Because ibmq_fez v1.3.30 has basis gate set $U\in\{CZ, I, R_x, R_z, R_{zz}, SX, X\}$, to match the instruction set architecture of the QPU, the circuit used to prepare the ansatz state is first transpiled to use the native gate set. Thus, to quantify the effect of decoherence and gate fidelity issues, we must analyze the circuit after transpilation. We will investigate the transpiled circuit used to prepare the ansatz state, which is shown in figure 12.

As indicated by figure 12, that the relevant gate error quantities pertain to R_z, $\sqrt{X}$ (SX), X, and CZ. Because R_z gates are implemented via virtual frame changes, there are no associated gate durations or errors. We are now only concerned with the number of $\sqrt{X}$, X and CZ gates, with error rates $\epsilon_{\sqrt{X}}$, ϵ_X, and ϵ_{CZ}, respectively (see table 2).

We categorize the total error into three categories of hardware limitations: decoherence effects, gate errors, and measurement errors. Beginning with decoherence effects, we observe that the transpiled circuit in figure 12 includes one CZ gate, two layers of $\sqrt{X}$ gates, and one X gate. Using the calibration data in table 2, the circuit execution time is

$$t_{\text{circ}} \approx t_{CZ} + 2(t_{\sqrt{X}}) + t_X = t_{2Q} + 3(t_{1Q}) = 68\text{ ns} + 3(24\text{ ns}) = 140\text{ ns} = 0.14\,\mu\text{s}. \tag{23}$$

Given the T_1 and T_2 times are 170 μs, 0.1%-level errors due to decoherence would be expected.

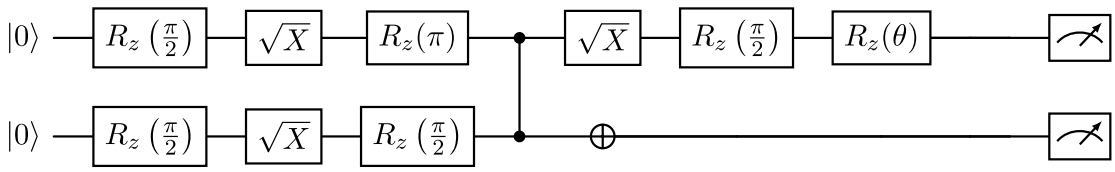

Figure 12. Transpiled circuit for measuring $\langle Z \otimes Z \rangle$. This circuit is ready for execution on ibmq_fez v1.3.30. Additional basis transformation gates are required for $\langle X \otimes X \rangle$ and $\langle Y \otimes Y \rangle$.

The total accumulated gate error ϵ_{gates} can be estimated from the errors of the physical operations in the circuit. The *CZ*, *SX* and *X* errors are listed in table 2. Adding these in quadrature for the number of physical gates gives $\epsilon_{\text{gates}} = 0.2\%$.

Lastly, summing the readout errors for qubit 131 and 132 in quadrature yields an estimated readout error 9%. This is an order of magnitude greater than the errors introduced by gate fidelity issues, and is the dominant error. Readout errors were mitigated by applying the twirled-readout method, which was achieved by setting noise resilience level 1 in Qiskit.

9. Conclusion and outlook

The hyperfine interaction is a spin–spin interaction that is important in atomic structure. We have implemented the hyperfine Hamiltonian $H = X \otimes X + Y \otimes Y + Z \otimes Z$ using the VQE algorithm and current NISQ hardware. An attractive feature of the hyperfine Hamiltonian is that it meets the requirements for the VQE algorithm, while also being a interesting spin–spin interaction typically found in physics problems, with an exact solution. A physically-motivated ansatz was developed that leads rapidly to convergence. The algorithm was implemented using a freely available graphical programming interface, and alternatively using either a simulator or a real quantum computer. Using Qiskit, classical optimization, and quantum error correction, rapid convergence was demonstrated using NISQ hardware.

Future directions for the research include expanding to higher-dimensional Hamiltonians, allowing further exploration of the relevance of spin degrees of freedom in atomic structure. Our main interest being the hyperfine interaction, we would like to study higher spin nuclei and higher electron angular momentum states. For example, the ground state of the Cs atom is $6^2S_{1/2}$ (notation: $N^{2S+1}L_J$) which has $I = 7/2$ and therefore splits into states with $F = 3, 4$ and the excited state $6^2P_{3/2}$ carries $F = 2, 3, 4, 5$ [14, 15]. The way that we treated the hyperfine interaction, states with half-integer *I* and *J* are easy to generalize into a hyperfine interaction of the form $\vec{I} \cdot \vec{J}$, since they result in even-dimensioned matrices ($4 \times 4, 6 \times 6, 8 \times 8, ...$) which are easy to write as strings of Pauli operators. For integer spins, e.g. $I = 1$, there are methods to encode these onto qubits as well [24]. A challenge when going to higher dimensional systems is that the number of possibilities for the Pauli strings can become large, which could present an issue for computation. We think that the best solution for these cases is likely to make use of the known symmetries of the system, starting in approximately the correct basis. It is known that for hyperfine interactions in alkali atoms, the F, m_F total spin basis is a good choice. We used this basis in section 6 to solve our smaller dimensional Hamiltonian exactly. We think that this basis could be used to study smaller corrections to the hyperfine splittings, leading to future improvements in precision for higher-dimensional systems.

In the present work, we selected an ansatz state that significantly restricted the Hilbert space exploration. This choice is appropriate when the symmetry of the ground state is known beforehand, but choosing such an ansatz state for an arbitrary Hamiltonian may limit convergence when the ground state lies outside the enforced symmetry [25]. In such a case, one may choose a more general, physics-agnostic ansatz state designed to suit the hardware, known as a hardware-efficient ansatz (HEA). Ansatzes categorized as hardware-efficient are typically designed to match the topology of the quantum device. HEAs would be an interesting topic to study for the case of higher-order corrections. While an HEA would certainly underperform our single-parameter ansatz, using the present simplified two-qubit Hamiltonian to study HEAs could be a very interesting next step for HEA studies.

Finally, the choice of the classical optimizer in this work was based on our good experiences with BOBYQA, especially given our restricted ansatz. We plan to expand our work to include SPSA, a common NISQ optimizer which would potentially require fewer function evaluations for convergence. It is likely that SPSA would improve the convergence, if additional ansatz parameters are opened up, which is likely to be necessary for higher dimensional systems.

Acknowledgments

The authors acknowledge the contributions of Prof. Dwight E. Vincent at The University of Winnipeg for help refocusing our work and for other useful discussions.

We acknowledge the use of IBM Quantum services for this work. The views expressed are those of the authors, and do not reflect the official policy or position of IBM or the IBM Quantum team.

JWM acknowledges the support of the Canada Research Chairs program and the Natural Sciences and Engineering Research Council of Canada (NSERC) SAPPJ-2023-00029.

Data availability statement

The data that support the findings of this study are openly available at the following URL/DOI: https://doi.org/10.5281/zenodo.18261447.

Author declarations

The authors have no conflicts to disclose.

References

[1] Armstrong L Jr 1971 *Theory of the Hyperfine Structure of Free Atoms* (Wiley)
[2] Peruzzo A, McClean J, Shadbolt P, Yung M H, Zhou X Q, Love P J, Aspuru-Guzik A and O'Brien J L 2014 A variational eigenvalue solver on a photonic quantum processor *Nat. Commun.* **5** 4213
[3] Tilly J *et al* 2022 The variational quantum eigensolver: a review of methods and best practices *Phys. Rep.* **986** 1
[4] McClean J R, Babbush R, Love P J and Aspuru-Guzik A 2014 Exploiting locality in quantum computation for quantum chemistry *J. Phys. Chem. Lett.* **5** 4368
[5] McArdle S, Endo S, Aspuru-Guzik A, Benjamin S C and Yuan X 2020 Quantum computational chemistry *Rev. Mod. Phys.* **92** 015003
[6] Dalton K, Long C K, Yordanov Y S, Smith C G, Barns C H W, Mertig N and Arvidsson-Shukur D R M 2024 Quantifying the effect of gate errors on variational quantum eigensolvers for quantum chemistry *npj Quantum Inf.* **10** 18
[7] Sweke R, Wilde F, Meyer J, Schuld M, Faehrmann P K, Meynard-Piganeau B and Eisert J 2020 Stochastic gradient descent for hybrid quantum-classical optimization *Quantum* **4** 314
[8] Higgot O, Wang D and Brierley S 2019 Variational quantum computation of excited states *Quantum* **3** 156
[9] Cadi Tazi L and Thom A J W 2024 Folded spectrum VQE: a quantum computing method for the calculation of molecular excited states *J. Chem. Theory Comput.* **20** 2491
[10] 2026 IBM Quantum Platform https://quantum.cloud.ibm.com
[11] Griffiths D J and Schroeter D F 2018 *Introduction to Quantum Mechanics* 3rd edn (Cambridge University Press) (https://doi.org/10.1017/9781316995433)
[12] Sakurai J J and Napolitano J 2020 *Modern Quantum Mechanics* 3rd edn (Cambridge University Press) (https://doi.org/10.1017/9781108587280)
[13] Cohen-Tannoudji C, Diu B and Laloë F 2020 *Quantum Mechanics, Volume II: Angular Momentum, Spin, and Approximation Methods* 2nd edn (Wiley-VCH Verlag GmbH & Co)
[14] Steck D A Cesium D Line Data http://steck.us/alkalidata (revision 2.3.4, 8 August 2025)
[15] Gerginov V, Derevianko A and Tanner C E 2003 Observation of the nuclear magnetic octupole moment of ^{133}Cs *Phys. Rev. Lett.* **91** 072501
[16] McMahon D 2008 *Quantum Computing Explained* 1st edn (Wiley-IEEE Computer Society Press) (https://doi.org/10.1002/9780470181386)
[17] Wong T 2022 *Introduction to Classical and Quantum Computing* 1st edn (Omaha, Nebraska, USA: Rooted Grove)
[18] Nielsen M A and Chuang I L 2010 *Quantum Computation and Quantum Information: 10th Anniversary Edition* (Cambridge University Press) (https://doi.org/10.1017/CBO9780511976667)
[19] 2025 IBM Quantum Composer https://quantum.cloud.ibm.com/composer
[20] Javadi-Abhari A *et al* 2024 Quantum computing with Qiskit arXiv:2405.08810v3
[21] Martin A J 2026 a-mart0/hyperfine-vqe: v1.0.0. Zenodo, https://doi.org/10.5281/zenodo.18261447
[22] Powell M J D 2009 *The BOBYQA algorithm for bound constrained optimization without derivatives, Technical Report* Cambridge University, Department of Applied Mathematics and Theoretical Physics
[23] Spall J C 1992 Multivariate stochastic approximation using a simultaneous perturbation gradient approximation *IEEE Trans. Autom. Control* **37** 332
[24] Getelina J C, Wang C-Z, Iadecola T, Yao Y-X and Orth P P 2024 Adaptive variational ground state preparation for spin-1 models on qubit-based architectures. *Phys. Rev. B* **109** 085128
[25] Kandala A *et al* 2017 Hardware-efficient variational quantum eigensolver for small molecules and quantum magnets *Nature* **549** 242